UDC 004.9: 53.08
DOI https://doi.org/10.32838/2663-5941/2019.3-1/35

***Chernetchenko D.V.***
Oles Honchar Dnipro National University

# A NOVEL METHOD OF PREPROCESSING AND SPIKE ENCODING OF ELECTROCARDIOGRAPHIC SIGNAL FOR MULTI-STABLE SPIKING NEURONAL NETWORKS APPLICATION

*Recent works in artificial intelligence propose that hardware and software solutions can be trained and taught instead of hard-coded algorithms. A key challenge for neural modeling is to explain how a continuous stream of multi-modal input from a rapidly changing sensory environment can be processed by artificial neuronal networks (ANN) in real-time. Our approach is based on a robust computational model of the spiking neuronal network (SNN) with multi-stable internal neurons. Investigated the applicability of the SNN model for the recognition of physiological signal patterns on noisy continuous input stream to extract common signal features of electrocardiographic signal (ECG). Number of detecting features was limited in this work only with QRS complex extraction and exactly R-peaks time position. One of the important challenge in signal data recognition relate to the quality of preprocessing and encoding method of input ANN's data. The novelty of our approach lies in using robust and effective raw-data preprocessing and encoding spatial-temporal properties of ECG signals directly into spike train and using this to excite recurrently connected spiking neurons in a SNN computation model; approach was developed, implemented and validated on real signals from MITDB and in-house ECG records. Also, efficiency of encoding input data stage was shown.*

***Key words:*** *electrocardiogram, artificial neuronal models, QRS detection, heart rate estimation, spiking neuronal networks, SNN.*

**Introduction.** Novel ways of programming by training, teaching, imitation and reward are already being demonstrated in portable devices with the help of in-silico chips behaving like neurons, i.e. neuromorphic chips [1; 2]. A central problem of such systems is the training of biological neural structures for a particular task and the implementation of the neural structure to the hardware system [3]. For the past decades, Artificial Neural Networks (ANN) have evolved to the point of being currently very close in behavior to biological neural structures [4−6]. In this paper, studied basic training problem of biological neural networks using a biologically realistic model of spiking neurons. A simple pattern recognition problem is applied to this model. Physiological pattern was chosen for recognition solution, this is electrocardiographic signal (ECG). Detection of ECG QRS complex provides fundamental feature for further detection of other waveforms and subsequent automatic analysis [7−9]. However, characteristics of ECG increase the difficulty of automatic ECG waveform detection [10]. Firstly, the morphology of ECG waveforms alters from person to person. Secondly, ECG signal frequently presents noise components of various origins. For example, the movement of patients' muscle can generate high-frequency noises and respiration may provoke baseline wander. Other noise components have electrical or mechanical origins. The recorded electrical data are often post-processed, either locally on the sensor [6] or on a device [7] attached to the sensor to estimate R-to-R peaks time intervals and heart rate. QRS pattern identification from ECG signal is fundamental approach to heart-rate estimation and heart rate variability (HRV) analysis [10]. Although QRS detection has achieved significant maturity over time [8], recent advances in wearable healthcare [5; 9] have motivated researchers to research QRS detection again. This is due to following facts: a) ECG readings from wearable sensors are contaminated with motion artifacts and baseline drifts; b) devices integrating wearable sensors are constrained in terms of area, power consumption and computational capabilities. In this work, spiking neural network (SNN) [11] with internal neurons multi-stability [19] for QRS complex detection and further R-to-R peaks intervals calculation was applied. Internal neurons multi-stability leads to capability of diverse spike regimes generation [13], such as spiking, bursting, oscillations, etc. Last works shows great efficiency of SNN. In [14], Maass draws a retrospective of the techniques used for modeling neural networks and presents the *third generation* of neural are spiking neuronal networks. Additionally, previous experience shows very good perspective for implementation of such neuronal system to the hardware architecture. But SNN's are still very sensitive to data representation form and quality of input signal. In this work we propose universal, easy to calculate and

integrate into hardware ECG raw-data preprocessing methodology and spike encoder for SNN implementation. To validate efficiency of proposed algorithms the recurrent SNN was built and results of detecting standard ECG signal QRS feature compared for cases with and without preprocessing stage. Also, system energy consumption of encoding and data processing method need to explore.

**Methods.** *Raw-data preprocessing*. The initial step of the ECG raw-data features extraction relates to the of noise removal from the signal. Noises from different origin always mix with ECG signal and cause baseline drifts, artifacts and small-scale oscillations. In this work, a cascaded digital filters configuration is used for removal of three major noises of baseline drift, power line interference and EMG noise [8−10]. Schematic diagram of preprocessing tract shows on Figure 1.

Each stage of filtration implemented with MATLAB environment. After common noise filtering, signal squared and processed with smoothing moving average filter (see Fig. 1). The squared and smoothed signal is good enough for accurate detection of peaks in ECG signal as well for deterministic methods and SNN approach. Firstly, low-pass filter designed with transfer function:

$$H(z) = \frac{\left(1 - z^{-6}\right)^2}{\left(1 - z^{-1}\right)^2}, \qquad (1)$$

The cutoff frequency is about 15 Hz, the delay is five samples, and the gain is 36. Figure 2*a* show the magnitude and phase responses of the corresponding low-pass filter. This filter can effectively decrease the noise which origin from the power supply interference (50/60 Hz noise), assume that the sampling frequency of ECG signalsis equal to 250 Hz. Also, high-pass filtering applied to the signal to decrease influence of noise with low frequencies components, such as baseline wondering or drift. High-pass filter designed with transfer function:

$$H(z) = \frac{\left(-1 + 32z^{-16} + z^{-32}\right)}{\left(1 + z^{-1}\right)}, \qquad (2)$$

The cutoff frequency of high-pass filter is 5 Hz. Figure 2*b* show the magnitude and phase responses of the corresponding high-pass filter. After high-pass filtration, raw-data processed with derivative filter with transfer function:

$$H(z) = \frac{1}{8T}\left(-z^{-2} - 2z^{-1} + 2z + z^2\right), \qquad (3)$$

By next step, signal squaring for nonlinearity enhance the dominance peaks and increase of signal to noise relation. Figure 3*a* shows example of squared ECG signal. At the last stage of data filtration squared signal is processed with moving average filter (MWI). A weighted moving average filter was used for the output signal smoothing [10].


**Fig. 1. Common block-diagram of ECG-signal filtration tract. Consist of: low-pass filter, high-pass filter, derivative filter, signal squaring, moving average filtration stage**

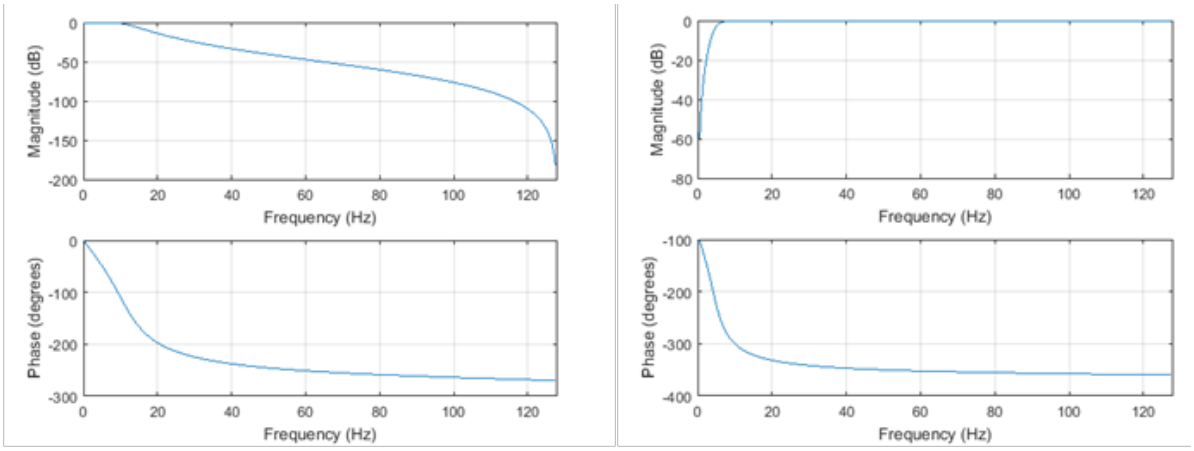


a b

**Fig. 2. *a* – magnitude (top) and phase (bottom) responses of ECG low-pass (LP) filter; *b* – for high-pass (HP) filter; x-axis frequency of signal in Hz; y-axis magnitude of signal in dB for magnitude response and Phase in degrees for phase response, respectively**

Signal is averaged to remove high frequency noise (0.150 seconds length):

$$Y(nT) = \frac{1}{N}\left[x\left(nT-(N-1)T\right)+x\left(nT-(N-2)T\right)+\ldots+x(nT)\right], \quad (4)$$

Result signal after MWI filtration of previously squared signal shown on Figure 3*b*.

*QRS features extraction.* Universal robust algorithm of QRS complex detection method was discovered. Method can be easily ported on hardware architecture. To solve this problem, robust modification of Pan-Tompkins [15, 16] QRS detection algorithm was proposed. At this point in the algorithm, previous steps have generated a roughly pulse-shaped waveform at the output of the signal, which shown on Fig.3*b*. The decision as to whether a pulse corresponds to a QRS complex is performed with an *adaptive thresholding* operation. When analyzing the amplitude of the MWI output, the algorithm uses two threshold values ($THR_{SIG}$ and $THR_{NOISE}$, appropriately initialized during a brief 2 second trainings phase) that continuously adapt to changing ECG signal quality. The first pass uses these thresholds to classify each non-zero sample (*CURRENT_PEAK*) as either signal or noise:

- If *CURRENT_PEAK*>$THR_{SIG}$, that location is identified as a QRS complex candidate and the signal level ($SIG_{LEV}$) is updated: $SIG_{LEV}$=0.125 **CURRENT_PEAK* + 0.875 * $SIG_{LEV}$.

- If $THR_{NOISE}$<*CURRENT_PEAK*< $THR_{SIG}$, then that location is identified as a noise peak and the noise level ($NOISE_{LEV}$) is updated: $NOISE_{LEV}$=0.125 **CURRENT_PEAK* + 0.875 * $NOISE_{LEV}$.

Based on new estimates of the signal and noise levels ($SIG_{LEV}$ and $NOISE_{LEV}$, respectively) at that point in the ECG, the thresholds are adjusted as follows: $THR_{SIG} = NOISE_{LEV} + 0.25 * (SIG_{LEV} - NOISE_{LEV})$. $THR_{NOISE} = 0.5 * THR_{SIG}$. These adjustments lower the threshold gradually in signal segments that are deemed to be of poorer quality. In the thresholding step above, if *CURRENT_PEAK*< $THR_{SIG}$, the peak is deemed not to have resulted from a QRS complex. However, an unreasonably long period has expired without an abovethreshold peak, the algorithm will assume a QRS has been missed and perform a search back. The minimum time used to trigger a search back is 1.66 times the current R-to-R peak time period. Also, it's impossible for a detect QRS complex if it lies within 200ms after a previously detected one with due to physiological refractory period.Example of detection processing show on Figure 4.

*Spike encoder.* Next important task is to create robust and efficient mechanism to encoding input analog signal to spiking sequence, which conduct directly to SNN inputs. Moreover, this implementation need to be very robust and easily to implement on hardware structures.

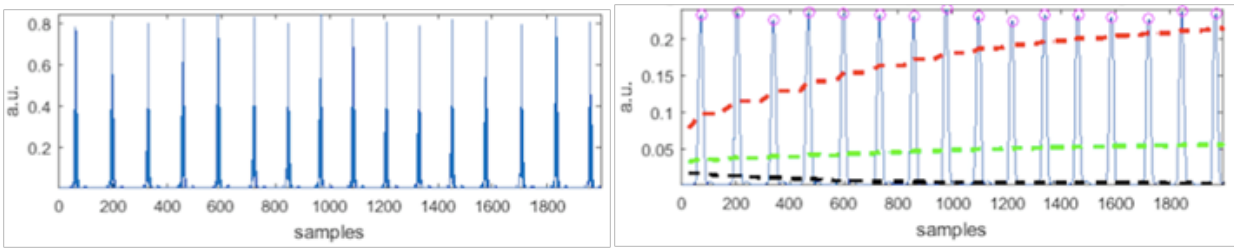


a b

**Fig. 3. *a* − squared normalized ECG signal after filtration stage; *b* − moving average filtration effect with detected R-peaks (circles) and detector levels (signal level – red dashed line; noise level – black dashed line; adaptive threshold – green dashed line). x-axis – samples number of signal; y-axis – amplitude of normalized signal in arbitrary units (a. u.)**

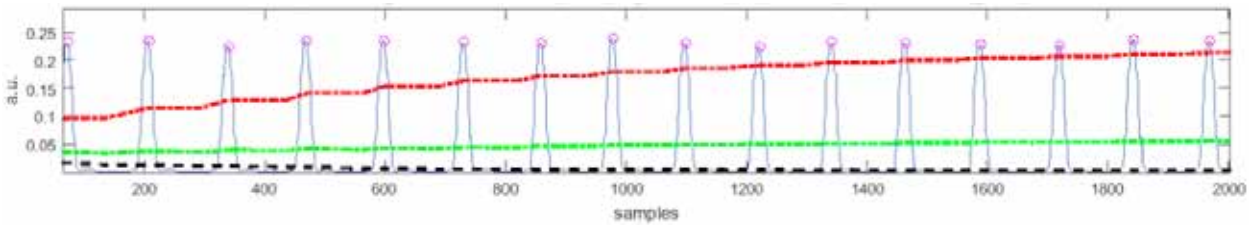


**Fig. 4. Detection of ECG QRS complexes and R-peaks timestamps with proposed deterministic reference algorithm. Circles highlight detected R-peaks timestamps, red dashed line – signal level; green dashed line – adaptive threshold; black dashed line – noise level. x-axis – signal sample number; y-axis – normalized signal amplitude in arbitrary units**

Temporal coding [17] encodes information as inter-spike intervals, capturing the spatio-temopral structure of the input signal. For ECG QRS detection, temporal characteristics around QRS complexes need to encoded as inter-spike intervals and therefore, temporal coding is adopted in this work [17]. The spike encoder encodes input ECG signal to inter-spike intervals using a combination of threshold modulators, voltage comparator, spike generator and a timer. To prevent aliasing effect, method of adapting the timer interval in response to the input waveform was realized. This will allow our SNN to better distinguish the two spike trains, further improving accuracy. One approach to adapt timer intervals is by setting its clock frequency to be proportional to the highest Fourier component extracted from the waveform. Clock frequency FCLK depends on the signal slope as peace-wise function with two saturation levels:

$$F_{CLK}\left(A_{f0}\right) = \begin{cases} F_{CLK\_min},\ F_{CLK} \le F_{CLKmin} \\ \frac{\left(F_{CLK\_max} - F_{CLK\_min}\right)}{k} * \left(A_{f0} - a\right) + F_{CLK\_min},\ F_{CLK\_min} < F_{CLK} < F_{CLK\_max} \\ F_{CLK\_max},\ F_{CLK} \ge F_{CLK\_max} \end{cases}, \quad (8)$$

where $F_{CLK\_max}$ maximum of timer clock frequency of timer, $F_{CLK\_min}$ minimum of timer clock frequency, $A_{f0}$ frequency of the input's signal most significant frequency harmonica (highest amplitude of non-DC peak of Discrete Fourier Transformation). Parameters *k* and *a* were constants during all simulations, relate to the certain frequency parameters of input ECG signals and let k=14.0 and a=1.0 Hz, respectively. Minimum timer clock frequency also constant and equal $F_{CLK\_min}$ =5 Hz, maximum frequency $F_{CLK\_max}$ varied from 100 to 1000 Hz for power consumption exploration.

The working principle of the spike encoder is described by following scenarios: a) ECG signal is rising; b) ECG signal is falling and c) ECG signal is stable within a time window Δ. The encoding is based on two thresholds $L_{thr}$ and $U_{thr}$ ($U_{thr}$>$L_{thr}$). Voltage comparisons are performed at a fixed interval controlled using the timer. At every interval, the comparator is enabled to compare the ECG voltage and the threshold $U_{thr}$. For simplicity, assume that the ECG signal is rising. The voltage comparison is positive, triggering the following sequence of events:

- threshold update: $L_{thr} = U_{thr}$ and $U_{thr} = U_{thr} + \Delta$;
- enable spike generator to emit one spike;
- restart timer and return to wait.

If the result of the comparison is negative (meaning the ECG signal is either falling or stable within Δ), a second comparison is performed, where the ECG voltage is compared with the threshold $L_{thr}$. If this comparison is positive and ECG signal is falling, the following sequence of events are triggered:

- threshold update: $U_{thr} = L_{thr}$ and $L_{thr} = L_{thr} - \Delta$;
- restart timer and return to wait.

If the result of the second comparison is also negative, when the ECG signal is stable within Δ, thresholds are not updated and timer is restarted. Following are the specific basicrules of this approach. a) Threshold updates are performed to track the ECG signal in the upward or downward directions. b) No spikes are generated when the ECG signal is falling. This is a design choice used in this work as the spatio-temporal characteristics of the QRS can be captured using the rising part of the voltage waveform. c) No spikes are generated if the ECG signal is stable.

*Spiking neuronal network.* The proposed neural network is a simulation of spiking neuronal network [18] based on multi-stable neurons, which occurs due to metrical asymmetry of active dendritic structure as shown before at [19]. Active spiking functionality of each neuron described by differential equations:

$$\begin{cases} v' = 0.04v^2 + 5v + 140 - u + I_0 \\ u' = a\left(bv - u\right) \end{cases}, \quad (9)$$

system reset to the initial state after spike generation:

$$if\ v \ge 30\,mV, then \quad \begin{cases} \mathrm{v} \leftarrow \mathrm{c} \\ \mathrm{u} \leftarrow \mathrm{u} + \mathrm{d}, \end{cases} \quad (10)$$

Each neuron has three-stable states due to their dendritic metrical asymmetry [19]. Stable states of internal neurons defined by the internal structure current distribution $I_0$ over the whole structure. Neuronal structure consists of three layers: input, recurrent and output. The first layer is the input layer, which generates spikes (encoded directly from the input ECG). The second layer is the recurrent layer and consists of $N = N_E + N_I$ recurrently connected neurons, where $N_E$ is the number of excitatory neurons and NI is the number of inhibitory neurons. Current framework consists of 1000 internal neurons with proportion $N_I = 0.25\ N_E$. Connections between two particular cells are arranged with probability calculated according to the rule:

$$P(D) = C * \exp\left(\frac{-D(A,B)}{\lambda}\right), \quad (7)$$

where D (A, B) stands for the Euclidean distance between two cells A and B, and λ is the density of connections. Parameter C depends on the type of pre-synaptic and postsynaptic neurons, that is, whether they are the excitatory (Ex) or inhibi-

tory (Inh) cells. In our simulations, the parameter C is set as: $C_{Ex-Ex}$ = 0.3 (for connections between two excitatory neurons), $C_{Ex-Inh}$ = 0.2 (for connections between excitatory and inhibitory neurons), $C_{Inh-Inh}$ = 0.1 (for connections between two inhibitory neurons), $C_{Inh-Ex}$ = 0.4 (for connections between inhibitory and excitatory neurons. Initial synaptic strengths $W_0$ = 0.0045 μSim/cm$^2$. Changes in synaptic strength are bounded between 0 and 10*$W_0$. Synaptic connection delays are selected randomly between 1ms and 2ms. The output level represented by two simple bi-stable neurons with active dendritic structure enhanced, which gather synaptic inputs from neurons of second layer and is able to generate single spikes in response to a large number of simultaneous spikes from recurrent neurons of second layer. One neuron which reacting when R-peak of QRS complex detected and second test neuron for comparison between learning and no stimulation. Output neuron work in following manner: generation of spike occurs only when R-peak of QRS complex was detected and no generate spike, when no QRS complex was detected. Synaptic weight updates are disabled after a time interval Ti. The time interval 0 (start of ECG sample) to Ti is training phase of the spiking neural network. In this phase, weights are updated using spike timing dependent plasticity (STDP). STDP is a rule for neurons to strengthen or weaken their connections according to their degree of synchronous firing [20, 21, 22, 23 ,24]. With the function W(x) defining the order of decrease or increase of strength depending on the synchrony of spiking between pre- and post-synaptic neurons, expressed in the following manner:

$$\Delta W = \begin{cases} A_+ \exp^{\left(\frac{\Delta t}{\tau_+}\right)}, \ for \ \Delta t > 0 \\ A_- \exp^{\left(\frac{\Delta t}{\tau_-}\right)}, \ other \ wise \end{cases}, \qquad (8)$$

All input ECG raw-data for network learning and QRS detection algorithm testing divide on two categories by the source: ECG signal database MITDB, and ECG signals which registered in-house in our laboratory with certified 12-lead ECG machine (CE, FDA). All samples from database was chosen randomly. Sampling frequency of input data was 250 Hz. Absolute values of amplitudes measure in μV. All simulations discussed in this paper were processed in the MATLAB environment.

**Results.** All results of the work can be separated on three main series ofexperiments. In first series, presented efficiency of QRS detection using signal pre-processing and deterministic algorithm, which was describe above. In second part, stability and efficiency of ECG signal encoder with help of proposed algorithm was estimated, third part connected to efficiency estimation of proposed SNN under presence of input preprocessing filtration and without.

To estimate an accuracy of proposed system for each RR interval extraction used Mean Average Percent Error (MAPE):

$$MAPE = \frac{1}{N}\sum_{i=0}^{N-1}\left(\frac{|a_i - p_i|}{a_i}\right) * 100, \qquad (11)$$

where MAPE calculated as absolute difference between the actual RR interval ai and estimated RR interval pi and N is the number of one-minute segments in the given ECG sample.

*a) Software signal features extractor validation.* Algorithm was successfully tested on 10 different ECG records with duration trimmed by 300 seconds. Signal necessary preprocessed with proposed above digital filtration (see Figure 1). Accuracy report and results of validation shown in Table 1. In our case, best case MAPE was 0.32% and worst case - 5.0%, respectively.

Table 1

**Accuracy results of reference method**

| # Record | Total beats | False Positive, # R-peaks | False Negative, # R-peaks | MAPE, % |
|---|---|---|---|---|
| 1 | 321 | 0 | 0 | 0.0 |
| 2 | 425 | 0 | 6 | 1.4 |
| 3 | 375 | 0 | 0 | 0.0 |
| 4 | 272 | 0 | 5 | 1.8 |
| 5 | 290 | 1 | 3 | 1.3 |
| 6 | 285 | 2 | 2 | 1.4 |
| 7 | 304 | 1 | 0 | 0.32 |
| 8 | 398 | 4 | 2 | 1.5 |
| 9 | 361 | 0 | 4 | 1.1 |
| 10 | 326 | 13 | 1 | 5.0 |

*b) QRS extraction with SNN.* Example of input-outputtime dependent relation for the output neuronal layer shown in Figure 6*a*. Need to add, that shown example could be named as case of well-trained network and results can be easily explained. Increasing of input spikes concentration on dendritic structure of output neuron leads to generation output spike, which explained aspresence of R-peak at certain moment of time in input signal. SNN's activity with time shown on Figure 6*b*. Extracted R-to-R intervals sequence shown on Figure 6*c*.

Figure 7 plots the comparative relation of average RR intervals estimation accuracy using SNN approach for five MITDB records and five internal

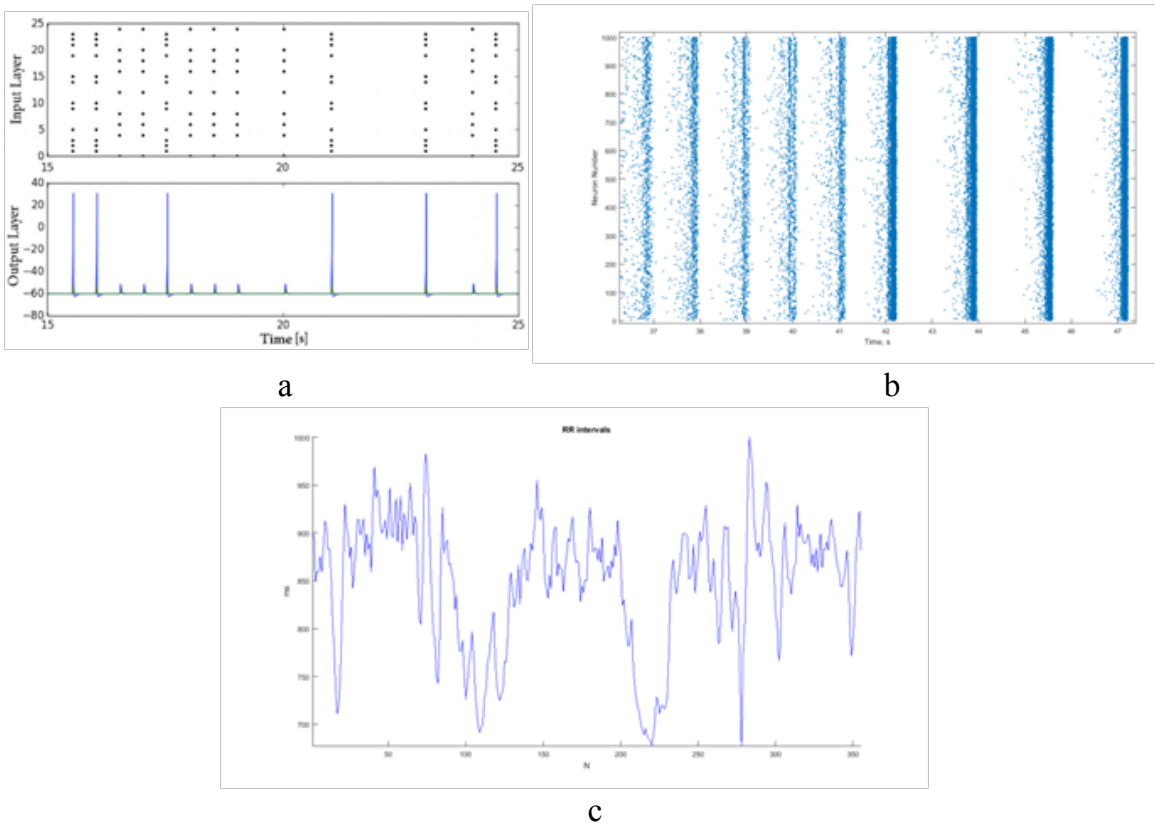


**Fig. 6. *a* − output neuron's activity registered form dendritic inputs (top), and output spike activity (bottom); *b* − general SNN neurons activity during 10 seconds time interval; c − R-to-R intervals sequence on SNN output**

records with presence of preprocessing stage and raw-data filtration, without filtration stage and estimation results with deterministic reference method. MAPE using our approach is less than 2% across all subjects. For our internal database, the MAPE varies between 0.5% and 2.1%, with an average of 1.2%. For MITDB database, the MAPE varies between 0.53% and 5.3%, with an average of 2.32%. Without filtration stage separation capability of SNN critically decrease, and MAPE varies between 2% and 12.2% with an average of 5%. The higher noises and artifacts level in input signal leads to higher increasing of MAPE for SNN.

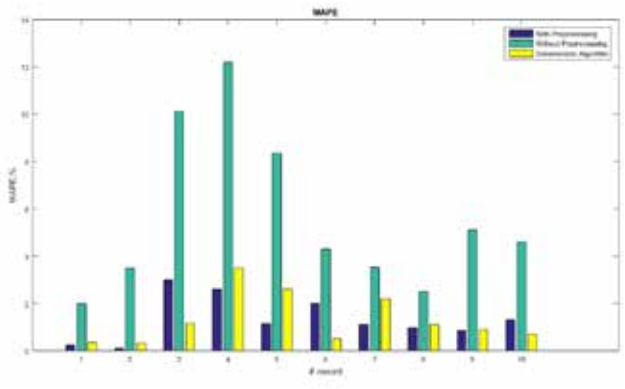


**Fig 7. MAPE values calculated for three main cases: purple bars − SNN results after learning stage and without any filtration; green bars – SNN results with preprocessing stage for input data; yellow bars – deterministic algorithm results**

*c) Spike encoder.* Figure 8 shows a zoomed part of the ECG signal and respective generated spike trains. The spike generation process from a segment of the ECG sample shown on bottom plot. Also highlighted in this figure are the regions of interest i.e., the QRS peaks. As discussed before and this can be seen quite well from this figure, spike temporal coding captures important spatio-temporal characteristics from the input signal in the form of inter-spike intervals.

Data density and energy consumption summary for six subjects from database shown in Table 2. Maximum clock timer of encoder varied 100, 500 and 1000 Hz, respectively. For each row item in the table, registered average spike firing rate (in Hz), the data density (bits per spike) and the energy consumption (in μW). The average spike firing rate is the total number of spikes generated in the SNN averaged over the ECG sample with duration 300 seconds. Data density measures efficiency of the spike encoder and is defined as:

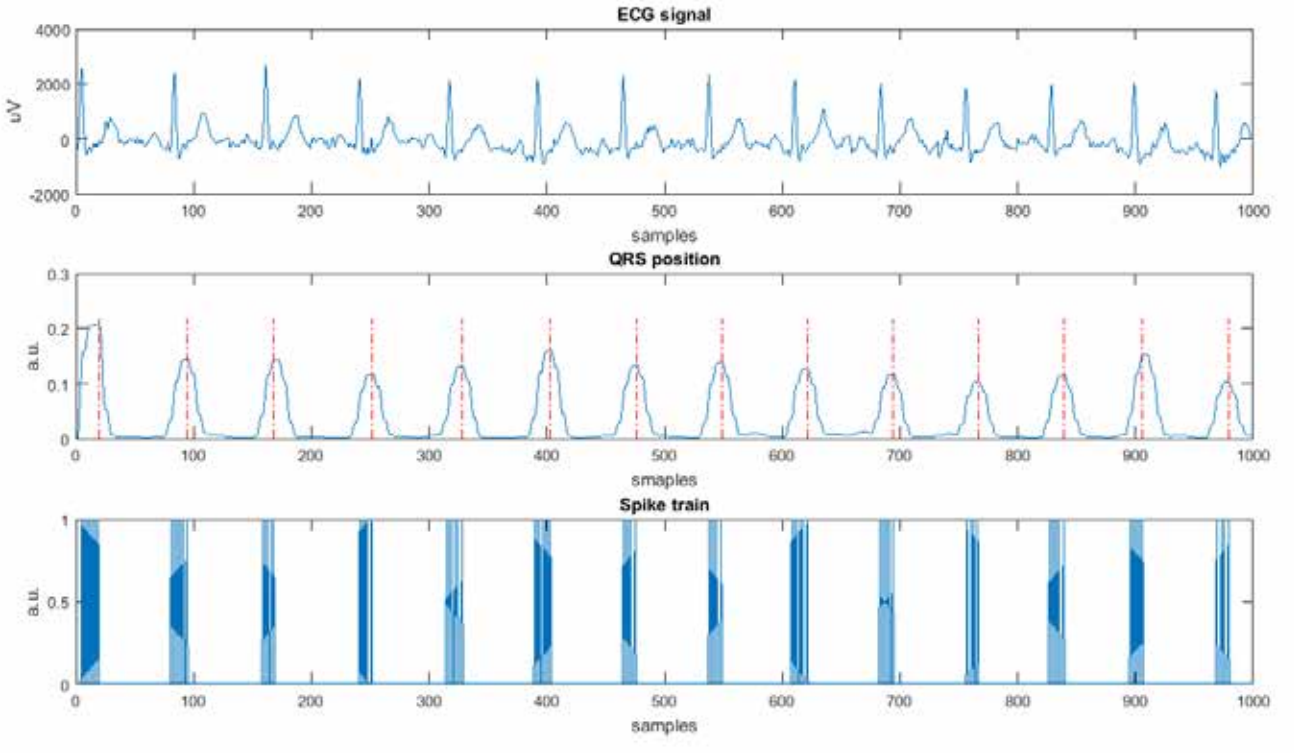


**Fig. 8. Zoomed part of the ECG signal and respective generated spike trains. Input signal shown on top plot; filtered and squared signal with R-peaks moments shown on middle plot; respective spike train generation with time shown on bottom plot. x-axis – sample number of signal; y-axis – input signal amplitude in uV (top), filtered signal and spikes normalized signals in arbitrary units (a. u.)**

$$Data\,density = \frac{ADC\,bits}{input\,spikes}, \qquad (12)$$

where input spikes parameter is the number of spikes generated at the output of our spike encoder (and input to the SNN) and ADC bits is the number of bits per ECG sample transmitted post analog to digital conversion (ADC).

The energy consumption of our approachestimating using methodology for FPGA structure generalpower consumption described in [21], at the constant normal ambient conditions and normal temperature. For fairness of comparison, the energy consumption using [25] excludes the ADC energy, while the energy consumption using ours exclude the spike encoder energy.

As seen from the table, the average data density (averaged over all subjects) for MITDB is 52.0 for $F_{CLK\_MAX}$=100 Hz. This result can be interpreted as follows: on average for every 52.0 bits of raw ECG data transmitted from the sensor for RR intervals detection using standard QRS-detection techniques, our spike encoder transmits one spike for the same purpose.

Table 2

**Total energy consumption of system**

| # Record | $F_{CLK\_MAX}$, Hz | Average spike firing rate, Hz | Data density, bits/spikes | Energy consumption, μW |
|---|---|---|---|---|
| 1 | 100 | 5.3 | 53.6 | 1.09 |
| 2 | 100 | 5.9 | 50.4 | 1.11 |
| 3 | 500 | 7.5 | 37.2 | 1.24 |
| 4 | 500 | 7.2 | 40.3 | 1.27 |
| 5 | 1000 | 10.4 | 25.53 | 1.41 |
| 6 | 1000 | 9.8 | 27.3 | 1.39 |

For the three cases, the average energy consumption of the subjects is1.1 μW (1.09 – 1.11 μW), 1.25 μW (1.24 – 1.27 μW) and 1.40 μW (1.39 – 1.41 μW), respectively. This compression saves energy and data-bandwidth. The higher the density, the higher the savings. Need to say, the average energy consumption using our approach (averaged over all subjects) for MIT database is 1.25 μW lower than [25], signifying the importance of our approach for power constrained portable devices.

**Conclusions.** The proposed SNN computational model offers flexibility by allowing implementation of clinically significant use-cases (as readouts) from the spatio-temporal properties of ECG integrated inside a network of spiking neurons. Solution of the QRS detection use-case was demonstrated. In future, we will investigate more ECG signal feature extraction. Additionally, the unsupervised readout is conducive to personalized healthcare, by allowing learning from subjects directly, without requiring costly data annotations to train the network. This allows future devices to be used seamlessly for subjects with and without cardiac irregularities. Our approach presents three novel contributions: (a) the technique to encode spikes from ECG directly, without requiring to digitize the analog ECG signal and thus achieving great reduction in data density; (b) preprocessed and filtered data at input increase SNN learning quality in a computation model and decrease output recognition error more than 4x times. Moreover, this can be efficiently implemented on FPGA hardware, with decreased energy consumption over existing hardware approaches; and (c) an unsupervised readout for RR intervals estimation case, where system have stable state as the whole when next R-peak occur. Additionally, the approach can be readily deployed to subjects with rare cardiac conditions, where ECG data is not always available to train a supervised classifier. These results suggest that our approach can be very well integrated in future hardware portable and wearable devices, providing significant battery life and improving user experience.

**References:**

1. Helleputte N. Van, Konijnenburg M., Pettine J., Jee D.-W., Kim H., Morgado A., Wegberg R. Van, Torfs T., Mohan R., Breeschoten A., et al., A 345 μw multi-sensor biomedical soc with bio-impedance, 3-channel ecg, motion artifact reduction, and integrated dsp. *IEEE Journal of Solid-State Circuits.* 2015. 50 (1). 230–244.

2. Krasauskas Z., Telksnys L. Ubiquitous personal heart rate long distance transmission to the treatment centers based on smart mobile phone application. *2015 IEEE 3rd Workshop on Advances in Information, Electronic and Electrical Engineering (AIEEE)*. 2015. Pp. 1–4. DOI: 10.1109/AIEEE.2015.7367297.

3. Ravanshad N., Rezaee-Dehsorkh H., Lotfi R., Lian Y. A level-crossing based qrs-detection algorithm for wearable ecg sensors. *IEEE Journal of Biomedical and Health Informatics*. 2014. №18 (1). 183–192.

4. Karimipour A., Homaeinezhad M.R. Real-time electrocardiogram p-qrs-t detectiondelineation algorithm based on quality-supported analysis of characteristic templates, Computers in Biology and Medicine. 2014. № 52. 153–165. DOI: https://doi.org/10.1016/j.compbiomed.2014.07.002.

5. Jain S., Ahirwal M., Kumar A., Bajaj V., Singh G. QRS detection using adaptive filters: A comparative study. *ISA Transactions*. 2017. № 66. PP. 362–375. DOI: https://doi.org/10.1016/j.isatra.2016.09.023.

6. Tekeste T., Saleh H., Mohammad B., Khandoker A., Elnaggar M. A nano-watt ecg feature extraction engine in 65nm technology. *IEEE Transactions on Circuits and Systems II: Express Briefs PP*. 2017. (99). 1–1. DOI: 10.1109/TCSII. 2017.2658670.

7. Arbateni K., Bennia A. Sigmoidal radial basis function ANN for QRS complex detection. *Neurocomputing*. 2014. № 145. PP. 438–450. DOI: https://doi.org/10.1016/j.neucom.2014.05.009.

8. Colgin L.L. Rhythms of the hippocampal network. *Nat. Rev. Neurosci*. 2016. V. 17. № 4. P. 239–249. DOI: 10.1038/nrn.2016.21.

9. Mizuseki K., Buzsaki G. Theta oscillations decrease spike synchrony in the hippocampus and entorhinal cortex. *Philos. Trans. R. Soc. Lond. B. Biol. Sci*. 2014. V. 369. № 1635. P. 20120530. DOI: 10.1098/rstb.2012.0530.

10. Schaffer J.D. Evolving spiking neural networks: A novel growth algorithm corrects the teacher. *Proc. of 2015 IEEE Symposium on Computational Intelligence for Security and Defense Applications (CISDA)*. May 26−28 2015. Pp. 1−8.

11. Yongqiang Cao, Yang Chen, Deepak Khosla. Spiking Deep Convolutional Neural Networks for Energy-Efficient Object Recognition. *Proc, of International Journal of Computer Vision*. May 2015. Volume 113. Issue 1. PP. 54−66.

12. Hunsberger E., Eliasmith C. Spiking Deep Networks with LIF Neurons. - arXiv: 1510.08829, 2015.

13. Diehl P.U., Neil D., Binas, J., Cook, M., Liu, S.C., Pfeiffer, M. Fast-Classifying, High-Accuracy Spiking Deep Networks Through Weight and Threshold Balancing. *Proc. of IEEE International Joint Conference on Neural Networks (IJCNN)*, 2015.

14. Kappel D., Nessler B., Maass W. STDP Installs in Winner-Take-All Circuits an Online Approximation to Hidden Markov Model Learning. *PLoS Comput. Biol*. 2014. Vol. 10. № 3. DOI: 10.1371/journal.pcbi.1003511

15. Pan J. and Tompkins W. J. A Real-Time QRS Detection Algorithm. *IEEE Transactions on Biomedical Engineering*. 1985. Vol. BME-32. No. 3. Pp. 230–236.

16. Hamilton P.S. and Tompkins W.J. Quantitative Investigation of QRS Detection Rules Using the MIT/BIH Arrhythmia Database. *IEEE Transactions on Biomedical Engineering*. 1986. Vol. BME-33. No. 12. Pp. 1157–1165.

17. Du D., Odame K. A bio-inspired ultra-low-power spike encoding circuit for speech edge detection. *Biomedical Circuits and Systems Conference (BioCAS)*, 2011 IEEE, IEEE. 2011. Pp. 289–292.

18. Izhikevich E.M. Simple model of spiking neurons. *IEEE Transactions on neural networks*. 2003. № 14 (6). PP. 1569–1572.

19. Snezhko E.M., Chernetchenko D.V. Dynamics of electrical potentials of neuron networks models with non-linear activation functions. *Vestnik DNU.* 2012.

20. Nam P., G.J. et al. "TrueNorth: Design and Tool Flow of a 65 mW 1 Million Neuron Programmable Neurosynaptic Chip". *IEEE Trans. Comput. Aided Des. Integr. Circuits Syst*. 2015. № 34. PP. 1537–1557. DOI: 10.1109/TCAD.2015.2474396.

21. Henderson J.A., Gibson T.A., Wiles J. Spike Event Based Learning in Neural Networks. – arXiv:1502.05777, 2015.

22. Kasabov N., Dhoble K., Nuntalid N., Indiveri G. Dynamic evolving spiking neural networks for on-line spatio- and spectro-temporal pattern recognition. *Neural Networks*. 2013. № 41. PP. 188–201.

23. Diehl P.U., Cook M. Unsupervised learning of digit recognition using spike timing-dependent plasticity. *Frontiers in computational neuroscience.* 2015. № 9 (0). 0–0.

24. Tavanaei A., Maida A.S. A spiking network that learns to extract spike signatures from speech signals. *Neuro computing.* 2017. № 240. PP. 191–199.

## НОВИЙ МЕТОД ПОПЕРЕДНЬОЇ ОБРОБКИ ТА ІМПУЛЬСНОГО КОДУВАННЯ ЕЛЕКТРОКАРДІОГРАФІЧНОГО СИГНАЛУ ДЛЯ ЗАСТОСУВАННЯ МУЛЬТИСТАБІЛЬНИХ СПАЙКОВИХ НЕЙРОННИХ МЕРЕЖ

*Нещодавні роботи з штучного інтелекту пропонують, щоб апаратні та програмні рішення можна було навчати і навчати замість жорстко закодованих алгоритмів. Ключовим викликом для нейронного моделювання є пояснення того, як безперервний потік мультимодальних входів із швидко мінливого сенсорного середовища може бути оброблений штучними нейронними мережами (ШНМ) в режимі реального часу. Наш підхід ґрунтується на надійній обчислювальній моделі спінної нейронної мережі (SNN) із мультистабільними внутрішніми нейронами. Досліджено застосовність моделі SNN для розпізнавання фізіологічних закономірностей сигналу на шумному безперервному вхідному потоці для вилучення загальних сигнальних особливостей електрокардіографічного сигналу (ЕКГ). Кількість виявлених ознак була обмежена в цій роботі тільки з екстракцією комплексу QRS і рівномірним положенням R-піків. Одним із важливих завдань у розпізнаванні даних сигналу є якість попередньої обробки та способу кодування вхідних даних ANN. Новизна нашого підходу полягає у використанні надійної та ефективної попередньої обробки сировинних даних та кодування просторово-часових властивостей сигналів ЕКГ безпосередньо в спайкових процесах і використання цього для збудження повторно пов'язаних спайкових нейронів в обчислювальній моделі SNN; був розроблений, впроваджений і перевірений на реальних сигналах із MITDB та внутрішніх записах ЕКГ. Також було показано ефективність етапу кодування вхідних даних.*

***Ключові слова:*** *електрокардіограма, штучні нейрональні моделі, детектування QRS, оцінка частоти серцевих скорочень, пікові нейронні мережі, SNN.*

## НОВЫЙ МЕТОД ПРЕДВАРИТЕЛЬНОЙ ОБРАБОТКИ И ИМПУЛЬСНОГО КОДИРОВАНИЯ ЭЛЕКТРОКАРДИОГРАФИЧЕСКОГО СИГНАЛА ДЛЯ ПРИМЕНЕНИЯ МУЛЬТИСТАБИЛЬНИХ СПАЕЧНЫХ НЕЙРОННЫХ СЕТЕЙ

*Последние работы по искусственному интеллекту предлагают, чтобы аппаратные и программные решения можно было обучать и обучать вместо жестко закодированных алгоритмов. Ключевым вызовом для нейронного моделирования является объяснение того, как непрерывный поток мультимодальных входов из быстро меняющейся сенсорной среды может быть обработан искусственными нейронными сетями (ИНС) в режиме реального времени. Наш подход основывается на надежной вычислительной модели спинной нейронной сети (SNN) с мультистабильными внутренними нейронами. Исследована применимость модели SNN для распознавания физиологических закономерностей сигнала на шумном непрерывном входном потоке для извлечения общих сигнальных особенностей электрокардиографического сигнала (ЭКГ). Количество выявленных признаков была ограничена в этой работе только с экстракцией комплекса QRS и равномерным положением R-пиков. Одной из важных задач в распознавании данных сигнала является качество предварительной обработки и способа кодирования входных данных ANN. Новизна нашего подхода заключается в использовании надежной и эффективной предварительной обработки сырьевых данных и кодирования пространственно-временных свойств сигналов ЭКГ непосредственно в спаечных процессах и использовании этого для возбуждения повторно связанных спаечных нейронов в вычислительной модели SNN, был разработан, внедрен и проверен на реальных сигналах с MITDB и внутренних записей ЭКГ. Также была показана эффективность этапа кодирования входных данных.*

***Ключевые слова:*** *электрокардиограмма, искусственные нейрональные модели, детектирования QRS, оценка частоты сердечных сокращений, пиковые нейронные сети, SNN.*